Journal of the Korean Nuclear Society
Volume 27, Number 4, August 1995

A Mechanistic Model for Forced Convective Transition Boiling of Subcooled Water in Vertical Tubes

K.W. Lee, S.J. Baik, S.K. Han, K.I. Joo, and J.Y. Yang
Korea Atomic Energy Research Institute
(Received December 29, 1994)

수직관내 미포화수의 강제대류 천이비등에 대한 역학적 모델

이광원 · 백세진 · 한상구 · 주경인 · 양재영
한국원자력연구소
(1994. 12. 29 접수)

Abstract

A mechanistic model for forced convective transition boiling has been developed to predict transition boiling heat flux realistically. This model is based on a postulated multi-stage boiling process occurring during the passage time of an elongated vapor blanket specified at a critical heat flux con dition. Between the departure from nucleate boiling (DNB) and the departure from film boiling (DFB) points, the boiling heat transfer is established through three boiling stages, namely, the macrolayer evaporation and dryout governed by nucleate boiling in a thin liquid film and the unstable film boiling. The total heat transfer rate during the transition boiling is the sum of the heat transfer rates after the DNB weighted by the time fractions of each stage, which are defined as the ratio of each stage duration to the vapor blanket passage time. The model predictions are compared with some available experimental transition boiling data. From these comparisons, it can be seen that the transition boiling heat fluxes including the maximum heat flux and the minimum film boiling heat flux are well predicted at low qualities/high pressures near 10 bar.

요 약

강제대류 천이비등 열유속을 보다 실제적으로 예측하기 위한 역학적 모델을 개발하였다. 이 모델은 가열된 벽면 근처를 어떤 기포기둥(Vapor Blanket)이 통과할 때 일어나는 다단계 비등과정 즉, 임계 기포기둥의 형성, 기포기둥밑의 미소액막(Macrolayer)의 기화 및 고갈, 그리고 얇은 기체막에서 일어나는 불안정한 막비등과정에 기초하였다. 핵비등이탈점(DNB)과 막비등이탈점(DFB)사이의 천이비등 곡선상의 열유속은 임계 기포기둥이 주어진 벽면을 통과할 동안 상기한 각 비등과정의 지속 시간비(Time Fraction)를 각 비등열유속에 곱한 후 그것을 합하여 정량화하였다. 이 모델의 예측치를 현재까지 발표된 문헌들에 나타난 실험치와 비교한 결과, 본 모델은 저건도 및 10 bar 근처의 고압조건의 실험치를 잘 예측하는 것으로 나타났다.

1. Introduction

Transition boiling is an intermediate heat transfer mode where the heated surface temperature is too high to maintain nucleate boiling but too low to maintain stable film boiling. In this boiling mode, an increase in surface tempearture usually results in a decrease in surface heat flux. The transition boiling region of the boiling curve is traditionally considered to be bounded by the critical heat flux (CHF) with the corresponding CHF temperature (this point is corresponding to the maximum heat flux point in the boiling curve) and by the minimum film boiling (MFB) heat flux with the corresponding MFB temperature (see Figure 1). However, the transition boiling boundaries may be determined on the phenomenological basis as the points "a" and "d" rather than the points "b" and "c", as shown in Figure 1. Point "a" indicates the departure from nucleate boiling (DNB), which is characterized by the appearance of unstable local dry spots on the heating surface. Point "d" shows the departure from film boiling (DFB) characterized by the appearance of unstable local cold spots on the heating surface. Kalinin et al. [1] took notice of the fact that the transition from nucleate to film boiling with increasing the wall superheat ΔT_w (or the opposite transition with decreasing ΔT_w) is gradual and smooth, and the maximum heat flux (MHF) and MFB heat flux are interior points of the transition boiling region. To investigate the transition boiling mechanism based on the various experimental observations [1, 2], this classification is considered more promising than the traditional one.

Recently, the practical interest in transition boiling has increased in connection with the safety analysis of nuclear reactors, especially with studies of hypothetical loss of coolant accidents (LOCA) as the design basis accident for light water reactors, and heat treatment of metals. Up to now, the experimental and theoretical studies have been plentifully performed for the transition boiling in pool boiling situations, but scarce in forced convective boiling situations. The comprehensive review of Kalinin et al. [1] and Auracher [2] of the transition boiling shows that the present knowledge about transition boiling mechanism is plentiful only for pool boiling situations. However, the forced convective transition boiling mechanism is poorly understood due to the inherent complexity of this phenomenon and the experimental difficulties. Consequently, available prediction methods are promising in the pool boiling situations but yield large discrepancies in the forced convective boiling situations due to their limitations caused by the difficulty in accounting for the various physical mechanisms in a single correlation and the lack of reliable data base.

Most of the prediction methods for transition boiling are based on Berenson's postulate [3] that transition boiling is a combination of unstable nucleate boiling and unstable film boiling, each of which alternatively exists at any given location on the heating surface. This can be formulated as,

$$q_{tb} = F_A\, q_l + (1 - F_A)\, q_v \quad , \tag{1}$$

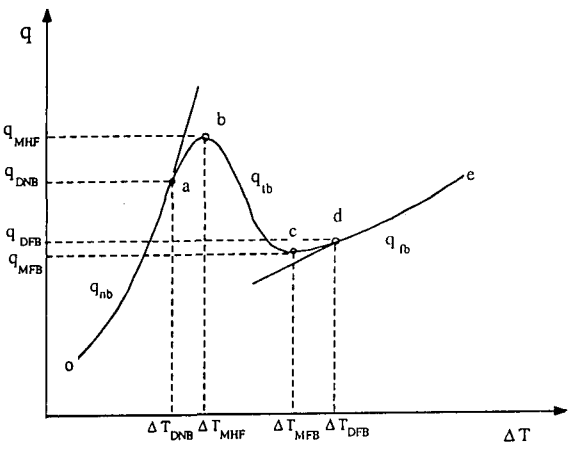

Fig. 1. Schematic Diagram for Transition Boiling Boundaries. Point (a): Nucleate Boiling Instability Boundary, Point (b): Maximum Heat Flux, Point (c): Minimum Film Boiling Heat Flux, Point (d): Film Boiling Instability Boundary

where, q_l and q_v designate the average heat fluxes during the liquid contact and the vapor contact, respectively. F_A denotes the average statistical fraction of the wetted area on the heated wall at a given moment. If the liquid-solid contact process can be assumed to be ergodic, the local liquid contact time fraction, F_T, is considered to be equal to the wetted area fraction, F_A.

Based on the idea of Equation (1), some phenomenological models for forced convective transition boiling have been developed by several investigators, such as Ragheb and Cheng [4], Bjornard and Griffith [5], and Kao and Weisman [6]. In the first two models, they assume that q_l and q_v are constant during the contact process, and equal to the MHF and the MFB heat flux of a boiling curve, respectively. They also assume that a linear relationship exists between the two anchor points and $F_A=1$ at the MHF point and $F_A=0$ at the MFB heat flux point, respectively. In these models, the expression of F_A becomes

$$F_A = \left(\frac{T_w - T_{MFB}}{T_{MHF} - T_{MFB}} \right)^2 , \qquad (2)$$

where, T_w, T_{MHF}, and T_{MFB} are the temperatures of the wall, MHF and MFB points, respectively. However, Kao and Weisman [6] introduced a moving quench front model to estimate the wetted area fraction (F_A) at high quality and low flow conditions, and used a wetted heat flux curve decreasing with temperature instead of a fixed MHF and a vapor convection heat flux instead of a fixed MFB heat flux, respectively, as two anchor points. In this model, the first anchor point is not the MHF point but the DNB point in the boiling curve (point "a" in Figure 1), thus the wetted area fraction at the MHF does not need to be unity.

In fact, the recent experimental studies [1, 2, 7−9] for the wetted area fraction show that F_A at the MHF is far below unity. Therefore, the correlations of the wetted area fraction derived from Equation (2) cannot be regarded as a reasonable estimate. Up to now, we cannot find reliable correlations for the estimation of the wetted area fraction in the forced convective boiling conditions, especially at low qualities/high flows. On the other hand, most of the recent theoretical studies on the transition boiling for pool boiling conditions, such as those of Kalinin et al. [1], Pan et al. [10], and Farmer et al. [11], assumed the liquid-solid contact process as a periodic sequence of transient conduction, nucleation and macrolayer dryout, and vapor film boiling phases on the heating surface. In these models, the wetted area fraction was evaluated by the liquid contact time fraction, assuming the contact process to be ergodic. These studies showed that the wetted area fraction at the MHF point was smaller than unity and the MHF is considerably higher than the steady state CHF value as the upper limit of nucleate boiling.

In this context, we attempt to develop a mechanistic prediction model for the forced convective transition boiling of subcooled water, based on the basic idea of Pan, Hwang, and Lin (PHL) theoretical model [10] for the pool boiling. For a specific feature of forced convective transition boiling, some mechanisms and assumptions in PHL model will be modified and their rationales will be discussed in the section of physical model and basic assumptions. The primary objective of this study is to predict the transition boiling heat flux properly, and to explain adequately the recent experimental evidence that the wetted area fraction at the MHF point is smaller than unity and the liquid contact heat flux is much higher than the CHF value.

2. Model Description

2.1. Physical Model and Basic Assumptions

Based on the previous investigations [10, 12−17] of the physical mechanisms of critical heat flux, transition boiling, and film boiling phenomena, the present physical model is supposed as depicted in Figure 2. For a complete transition boiling cycle, there are four key boiling stages, namely, approaching of vapor blanket, macrolayer evaporation, macrolayer dryout, and unstable film boiling with frequent liquid-solid contacts.

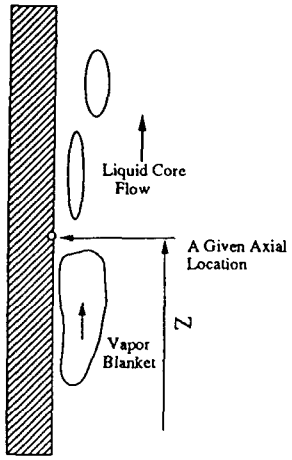

A. Approaching of Vapor Blanket

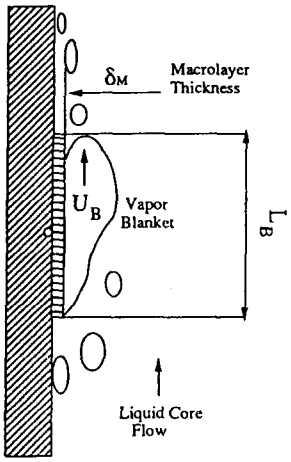

B. Macrolayer Evaporation under Vapor Blanket

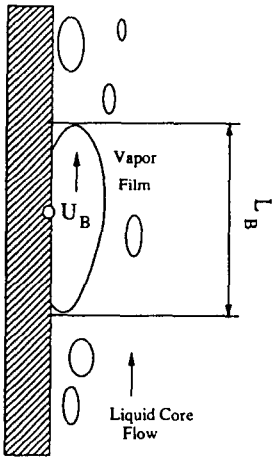

C. Macrolayer Dryout

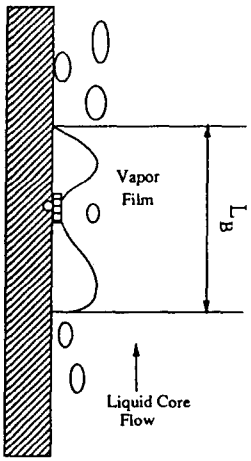

D. Unstable Film Boiling: Interfacial Wave Touches The Heated Wall

Fig. 2. Illustration of the Physical Model for Each Stage of Transition Boiling Cycle

It is assumed that the transition boiling cycle starts when a vapor blanket approaches to a given axial point on the heated wall. The DNB occurs when the macrolayer dryout time is equal to the vapor blanket passage time, which is determined by dividing the vapor blanket length, L_B, by the blanket velocity, U_B, at a CHF condition. Before the DNB, the heat transfer through the macrolayer is governed by a fully developed nucleate boiling. After the DNB, the wall heat transfer is established through two boiling stages, i.e., the macrolayer evaporation governed by a nucleate boiling in thin liquid film and the unstable film boiling with alternate wet and dry periods induced by the instability of the liquid and vapor interface. The present model assumes that the total heat transfer rate during the transition boiling is the sum of the

heat transfer rates after the DNB weighted by the time fractions of each stages, which are defined as the ratio of each stage duration to the vapor blanket passage time. The transition boiling heat transfer is terminated when the wall superheat exceeds the DFB temperature characterized by a complete separation of the liquid-vapor interface from the wall. From the assumed ergodicity of the time sequential process during the vapor blanket passage over a given point, the transition boiling heat flux at a given axial location can be estimated.

This physical model is similar to that of PHL pool boiling model [10], but it is considerably modified to accommodate the specific feature of forced convective situations. PHL model was based on three contributors of the transition boiling process, i.e., transient conduction, macrolayer evaporation, and vapor film boiling. In the present model, the effect of transient conduction on the forced convective transition boiling is assumed negligible and the vapor film boiling stage is replaced by the unstable film boiling stage due to the instability of the vapor-liquid interface under the forced convective boiling in the vertical tube geometry. To satisfy the ergodicity of the transition boiling process, the controlling phenomena are selected as a time sequential process occurring at a given point during the vapor blanket passage, instead of the controlling phenomena under the hovering bubble on the heated surface of PHL model. If the specified vapor blanket characteristics (its size, length, and velocity) are suitable as compared with the tube diameter and length, and the time scale including all the controlling phenomena, the ergodicity will be satisfied.

The present model is also similar to that of Katto, Yokoya, and Yasunaka (KYY) [17] for the pool transition boiling process. In KYY proposal, the bubble departure period specified at a CHF condition does not vary during the transition boiling process and the liquid macrolayer evaporation is the same as the nucleate pool boiling. Therefore, the DNB occurs when the liquid macrolayer dryout time is equal to that for the bubble departure time, and the heat flux after the DNB is determined by multiplying the wetting time fraction by the nucleate pool boiling heat flux. In this approach, the boiling curve slope of transition boiling region is too steep. This problem is overcome in the present model by introducing a new boiling mechanism in a very thin liquid film after the DNB and considering the strong contribution of an unstable film boiling on the total transition boiling heat flux in the forced convective boiling situations.

Katto [12], Lee and Mudawwar [13], and Mudawwar et al. [14] have developed a theoretical CHF model under subcooled flow boiling based on the similar physical mechanism. They have claimed that the crucial CHF mechanism of subcooled flow boiling is a macrolayer dryout under an elongated vapor blanket. In the present model, this mechanism is used for the determination of the DNB condition.

Ueda and Kim[15] and Hino and Ueda[16] investigated heat transfer characteristics near the CHF condition in a subcooled flow boiling system. They concluded that the wall temperature excursion at the CHF condition was composed of the temperature fluctuations which accompany periodic passing of large coalescent bubbles close to the surface and a subsequent sharp temperature rise under a film boiling state. Since this heat transfer characteristics is similar to that of transition boiling, the macrolayer behaviour under the vapor blanket is also thought to be a very important heat transfer mechanism in the transition boiling process.

After the DNB condition (point "a" in Figure 1), the macrolayer dries out before the vapor blanket passage time due to the thin film boiling heat flux which is higher than the CHF. Therefore, the macrolayer evaporation stage can contribute to the transition boiling heat flux in proportion to the macrolayer dryout time fraction to the vapor blanket passage time. Just after the macrolayer dryout, the wall surface is covered by thin vapor film. At this time, a depression in the vapor-liquid interface occurs due to the insufficient vapor generation and it allows the

interface to touch the dry wall surface if the wall temperature is below the DFB temperature (point "d" in Figure 1). This touching results in a vigorous boiling at the wall surface and then the interface is repulsed from the wall. This sequence is periodic, repeating itself and lasts until the vapor blanket passes a given point. In this model, the heat transfer characteristics of this sequence is evaluated by the simple thermomechanical model for the unstable film boiling proposed by Huang et al. [18]. The unstable film boiling period is determined by subtracting the macrolayer dryout time from the vapor blanket passage time.

The basic assumptions for the mathematical formulation of the physical model are listed below:

(1) The time sequential process occurring at a given point during the vapor blanket passage is ergodic.
(2) The vapor blanket passage time specified at the CHF condition remains constant with increasing the wall superheat, ΔT_w ($=T_w-T_{sat}$).
(3) The average length and velocity of the vapor blanket during the unstable film boiling period does not vary.
(4) The thermal and physical properties at a given point are determined at the CHF condition.

2.2. Mathematical Formulations of Physical Model

A. Critical Heat Flux and Vapor Blanket Characteristics

In the present physical model, the CHF condition for the forced convective boiling at low qualities reaches when the macrolayer dryout time is equal to the vapor blanket passage time. Based on the previous works of Katto [12], Lee and Mudawwar [13], and Mudawwar et al. [14], the CHF and the vapor blanket characteristics, i.e., its size, length, and velocity, are determined as follows.

From the mass balance on vapor stems in the macrolayer beneath the vapor blanket, each phase velocity is related as,

$$\rho_g U_g A_g = \rho_f | U_f | (A - A_g), \tag{3}$$

where, A and A_g denote the total surface area beneath the vapor blanket and the cross-sectional area of vapor stems, respectively. ρ_g, ρ_f, U_g, and U_f are the densities of vapor and liquid phases and the velocities of vapor and liquid phases, respectively. This equation simply means that there is a balance between the vapor outflow and the liquid inflow in the macrolayer. The vapor velocity is obtained by the energy balance on the vapor stem as follows:

$$q_B A = \rho_g U_g A_g h_{fg} , \tag{4}$$

where, h_{fg} is a latent enthalpy of vaporization and q_B is a boiling heat flux for vaporization, which is given as

$$q_B = q_{chf} - q_{sc} . \tag{5}$$

Here, q_{chf} is the total wall heat flux corresponding to a CHF and the subcooled liquid convective heat flux, q_{sc}, given by Shah's correlation for high flux boiling condition [20], can be expressed as

$$q_{sc} = \frac{230\, q_{chf}\, (q_{chf}/Gh_{fg})^{0.5}\, (T_{sat} - T_{lc})}{[230\,(q_{chf}/Gh_{fg})^{0.5} - 1]\, (T_{sat} - T_{lc}) + q_{chf}/H_{fc}}, \tag{6}$$

where, G is the mass flux and the single phase forced convective heat transfer coefficient, H_{fc}, is given by the well-known Dittus-Boelter correlation for turbulent flow. T_{sat} and T_{lc} are the saturation temperature and the subcooled water temperature, respectively. The allowable relative velocity in vapor stem can be evaluated by the Helmholtz instability criterion as follows:

$$(U_g - |U_f|)^2 = 2\pi\sigma(\rho_f + \rho_g)/(\rho_f \rho_g \lambda_H), \tag{7}$$

where, σ and λ_H are the surface tension and the wave length of Helmholtz instability, respectively. The thickness of the macrolayer at the CHF condition is assumed by Haramura and Katto [19] as follow:

$$\delta_{chf} = \lambda_H / 4. \tag{8}$$

From Equations (3), (4), (7) and (8), the macrolayer thickness can be rewritten as;

$$\delta_{chf}=\frac{\frac{\pi}{2}(1+\rho_f/\rho_g)\sigma(A_g/A)^2}{\left[1+(\rho_f/\rho_g)\frac{A_g/A}{1-A_g/A}\right]^2\rho_g\left(\frac{q_B}{\rho_g h_{fg}}\right)^2}, \quad (9)$$

where, A_g/A is given by Haramura and Katto's correlation [19] as follows:

$$A_g/A \quad (10)$$
$$=0.0654\left[(11\rho_f/16\rho_g+1)^{\frac{3}{5}}/(\rho_f/\rho_g+1)\right]^{\frac{1}{2}},$$
$$\approx 0.0584(\rho_f/\rho_g)^{0.2} \quad \text{for } \rho_f/\rho_g \gg 1.$$

The CHF condition occurs when the liquid supply into the macrolayer from the core flow is completely vaporized and can be formulated as follows:

$$L_B q_{chf}=\rho_f(U_B-U_M)\delta_{chf}h_{fg}[1+(h_f-h_{lc})/h_{fg}](1-A_g/A), \quad (11)$$

where, L_B and U_B are the length and velocity of the vapor blanket, respectively. And U_M is the macrolayer velocity, which is assumed nearly zero. h_f and h_{lc} are the enthalpies of saturated and subcooled liquids, respectively. The vapor blanket length can be determined by introducing Helmholtz instability criterion between the macrolayer and the vapor blanket, thus

$$L_B=2\pi\sigma(\rho_f+\rho_g)/[\rho_f\rho_g(U_B-U_M)^2]. \quad (12)$$

Since the macrolayer velocity is negligible as compared with the vapor blanket velocity, the relative velocity can be considered equal to the vapor blanket velocity. The vapor blanket velocity can be written from the force balance between buoyancy and drag force on the vapor blanket as follows:

$$U_B=\sqrt{2L_B g(\rho_{lc}-\rho_g)/\rho_{lc}C_D}+U_{bl}, \quad (13)$$

where, U_{bl} and C_D are the liquid alone velocity (or two-phase mixture velocity) at the mass center of vapor blanket and the drag coefficient of the vapor blanket, respectively. And ρ_{lc} is the density of subcooled water. If the liquid alone flow is turbulent, the liquid alone velocity, U_{bl}, can be obtained by the well-known Karman's three layer velocity profile. If the liquid alone flow is laminar, U_{bl} can be determined by,

$$U_{bl}=2G/\rho_{lc}[1-(R_o-y_B)^2/R_o^2]. \quad (14)$$

Here, R_o is the radius of tube and the distance of the vapor blanket center from the wall, y_B, is

$$y_B=\delta_{chf}+D_b/2. \quad (15)$$

The vapor blanket diameter, D_b, is assumed equal to the bubble diameter at the bubble detachment point. The correlations for the drag coefficient, C_D, and the vapor blanket diameter, D_b, will be discussed in the section of the constitutive equations. Consequently, the CHF is obtained by Equation (11) and the vapor blanket characteristics are determined by Equations (12) and (13).

B. Macrolayer Evaporation

Before the DNB, the macrolayer thickness is larger than that for the CHF condition (δ_{chf}) and the heat transfer through the macrolayer can be evaluated by the fully developed nucleate boiling heat flux, which is estimated by the correlation of Mikic and Rohsenow [21]. Fujita and Ueda [22] experimentally showed that the surface heat flux in falling liquid film approaches to a pool boiling heat flux as the wall superheating increases. From Mikic and Rohsenow's correlation for water boiling data [21], the fully developed nucleate boiling heat flux is expressed in SI units as follows:

$$q_{nb}=\frac{1.89\ 10^{-14}\sqrt{gx_f}\,(\rho_g h_{fg})^{1/8}\rho_f^{17/8}c_{pf}^{19/8}\Delta T_w^3}{\sigma^{9/8}(\rho_f-\rho_g)^{5/8}T_{sat}^{1/8}}, \quad (16)$$

where, κ_f and c_{pf} are the thermal conductivity and specific heat of saturated liquid, respectively. After the DNB, the macrolayer becomes thinner than that for the CHF condition (δ_{chf}), and the heat transfer through the macrolayer is changed from fully developed nucleate boiling to a thin film boiling. This thin film boiling is very different from the pool boiling or forced convective boiling. Mesler [23] suggested that the nucleate boiling heat flux in a thin liquid film might

be exceptionally high because a bubble generated in the thin film can escape quickly with a very small resistance. Kopchikov et al. [24] developed a correlation for the thin film boiling heat transfer focussed on the heat transfer through the quasi-laminar layer adjacent to the growing bubble. This correlation is expressed as,

$$q_{mb} = \frac{C x_f h_{fg} \rho_g \rho_f \Delta T_w^2}{\sigma T_{sat} (\rho_f - \rho_g)} , \quad (17)$$

where, C is an empirical constant, which is given as 0.01 for various fluids including water at the atmospheric and subatmospheric pressures. Kopchikov et al. [24] also explained that the boiling heat flux in a thin film boiling could increase up to the heat flux associated with the limiting temperature of the liquid superheat (i.e., Leidenfrost temperature), since in thin film boiling there are practically no hydrodynamic restrictions on the removal of the vapor and supply of the liquid.

Beattie and Lawther [25] investigated the structural change in a thin annular film as dryout is approached, and developed a more generalized thin film boiling heat flux equation based on the heat transfer through a single close-packed hexagonal layer of bubbles. If "N" bubble layers exist in the thin film, the boiling heat flux is given by

$$q_{mb} = \frac{0.0288 x_f h_{fg} \rho_g \rho_f \Delta T_w^2}{N \sigma T_{sat} (\rho_f - \rho_g)} . \quad (18)$$

It can be seen that the Beattie and Lawther correlation (Eq. 18) is equivalent to that of Kopchikov et al. if N is assumed to be 2. In the present model, the boiling heat flux in the macrolayer after the DNB is determined by Equation (18) with N=2 for the pressure below 110 kPa and N=3 for the pressure higher than 110 kPa. For the pressures higher than 110 kPa, the selection of higher "N" value is to consider the effect of the pressure on the packing of bubble layers in the macrolayer.

The DNB wall temperature can be determined by rearranging Equation (16) after substituting the CHF [Eq. (11)] for the nucleate boiling heat flux, q_{nb}. The step change in the macrolayer evaporation heat flux before and after the DNB temperature is treated as follows :

$$q_{me} = q_{nb} \quad \text{for } \Delta T_{sat} < \Delta T_{DNB} , \quad (19)$$

$$q_{me} = q_{mb}\{\Delta T_w\} + q_{chf} - q_{mb}\{\Delta T_{DNB}\} \quad \text{for } \Delta T_{DNB} < \Delta T_w < \Delta T_{DFB} , \quad (20)$$

$$q_{me} = 0 \quad \text{for } \Delta T_w > \Delta T_{DFB} , \quad (21)$$

where, $q_{mb}\{\Delta T_{DNB}\}$ and $q_{mb}\{\Delta T_w\}$ denote the macrolayer boiling heat fluxes determined by Equation (18) as the functions of the wall superheats ΔT_{DNB} and ΔT_w, respectively. Equation (20) means that the macrolayer boiling heat flux after the DNB starts from the CHF value (q_{chf}) and varies with the slope of Equation (18) up to the DFB point. The macrolayer thickness, δ_{me}, during the macrolayer evaporation stage can be evaluated by replacing the boiling heat flux, q_B, in Equation (9) with the macrolayer evaporation heat flux, q_{me}, determined by Equations (19) to (21). This thickness is distinguished from the CHF macrolayer thickness, δ_{chf}, of Equation (9). Finally, the macrolayer dryout time is given by,

$$\tau_{md} = \rho_{lc} \delta_{me} h_{fg} [1 + (h_f - h_{lc}) / h_{fg}] / q_{me} , \quad (22)$$

and the contribution of the macrolayer evaporation during the macrolayer dryout time to the total boiling heat flux is

$$\overline{q_{me}} = q_{me} \tau_{md} / \tau_p , \quad (23)$$

where, τ_p is the vapor blanket passage time, which is defined as,

$$\tau_p = L_B / U_B . \quad (24)$$

C. Unstable Film Boiling

Within the vapor blanket passage time, the macrolayer dries out, and then the heat transfer through a vapor film is available during the vapor film covering time. The vapor film covering time is defined as,

$$\tau_{vc} = \tau_p - \tau_{md} . \quad (25)$$

During the vapor film coverage time, the unstable film boiling with alternate dry and wet periods is established due to the instability of the vapor-liquid interface, which is augmented by a repeating insufficient and violent vapor generation under the vapor film. Therefore, the information for the interface contact frequency, size, and time is needed to quantify the heat transfer characteristics of the unstable film boiling. Up to now, this information for the forced convective boiling situations is unavailable in the literature.

In this model, the unstable film boiling heat transfer is simply evaluated by the thermomechanical model proposed by Huang et al. [18]. They developed an equation of the evaporation enthalpy between the wetting zone and dry zone, based on the conservation equations at the vapor-liquid interface. In their model, the wetting liquid on the highly heated wall is assumed to be at saturated state at an elevated pressure defined as the saturation pressure corresponding to the wall temperature. Also, the vapor is assumed to be saturated at the system pressure of the bulk liquid. The resulting equation is

$$h_g - h_f(T_w) = 0.5[\rho_f(T_w) - \rho_g] [p_s(T_w) - p]/\rho_g\rho_f(T_w) + (q_l^* - q_v^*)/m \quad (26)$$

where, p, $h_f(T_w)$, $\rho_f(T_w)$, and $p_s(T_w)$ designate the system pressure and the saturated liquid enthalpy, density, and pressure corresponding to the wall temperature, respectively. And q_l^*, q_v^*, and "m" are defined as

$$q_l^* = q_l + m V_l(V_g - V_i) , \quad (27)$$

$$q_v^* = q_v + m V_g(V_g - V_i) , \quad (28)$$

$$m = \rho_g(V_g - V_i) = \rho_f(V_l - V_i) , \quad (29)$$

where, q_l and q_v are heat fluxes from liquid phase to interface and from vapor phase to interface, respectively. V_l, V_g and V_i denote the liquid and vapor velocities normal to interface and the interface velocity, respectively. Equation (26) can be interpreted as the fact that the evaporation enthalpy is provided by both heat conduction and the mechanical energy released during the depressurization process of evaporation. Since the vapor is assumed at saturated state, q_v^* in Equation (26) must be zero to keep the vapor at the saturation temperature. If we assume that q_l^* is negligible near the DFB temperature, Equation (26) can be rewritten as,

$$h_g - h_f(T_{DFB}) = 0.5[\rho_f(T_{DFB}) - \rho_g] [p_s(T_{DFB}) - p]/\rho_g\rho_f(T_{DFB}). \quad (30)$$

Equation (30) is used to determine the DFB temperature and means that the evaporation enthalpy at the DFB point is supplied by the mechanical energy of depressurization alone. From the assumption that the wall heat flux during the unstable film boiling is proportional to the liquid heat flux at the interface, the following equation is derived,

$$q_{fb} = C_A q_l^* = m C_A\{h_g - h_f(T_w) - 0.5[\rho_f(T_w) - \rho_g] [p_s(T_w) - p]/\rho_g\rho_f(T_w)\}. \quad (31)$$

To remove the proportional coefficient, C_A, the DNB point is selected as the anchor point and then we can obtain the following equation :

$$\frac{q_{fb}}{q_{dnb}} = \frac{\{h_g - h_f(T_w) - 0.5[\rho_f(T_w) - \rho_g] [p_s(T_w) - p]/\rho_g\rho_f(T_w)\}}{\{h_g - h_f(T_{DNB}) - 0.5[\rho_f(T_{DNB}) - \rho_g] [p_s(T_{DNB}) - p]/\rho_g\rho_f(T_{DNB})\}} \quad (32)$$

For zero heat flux, Equation (32) reduces to Equation (30) for the DFB temperature. Finally, the contribution of the unstable film boiling to the total boiling heat flux is given as,

$$\overline{q_{fb}} = q_{fb}\tau_{vc}/\tau_p . \quad (33)$$

D. Boiling Curve Generation

In the present model, the boiling curve ranging from a nucleate boiling region to the DFB point can be generated. When the wall superheat is lower than

the DNB temperature or the macrolayer dryout time is shorter than the vapor blanket passage time, the total boiling heat flux is

$$q_t = q_{nb} \ . \tag{34}$$

Between the DNB point and the DFB point, the total boiling heat flux is

$$q_t = \overline{q_{me}} + \overline{q_{fb}} \ . \tag{35}$$

Equation (35) involves the DNB heat flux, the MHF and the DFB heat flux in the boiling curve. If the liquid contact time during the vapor coverage period is assumed negligible, the time fraction of liquid contact is given as,

$$F_T = \tau_{md} / \tau_p \ . \tag{36}$$

If the liquid contact process is ergodic, the following equality can be applied.

$$F_A = F_T \ . \tag{37}$$

2.3. Constitutive Equations

For the determination of the CHF and the vapor blanket characteristics, the subcooled flow boiling model is required. In the subcooled flow boiling model, the subcooling at the bubble detachment point, (h_f-h_{ld}), is very important in determining the position of bubble detachment and actual quality profile. To evaluate the liquid enthalpy at the bubble detachment point (h_{ld}), the well-known Saha and Zuber correlation described in Reference [26] is chosen as the best one for low pressure and low velocity conditions because this correlation can be applicable to laminar and turbulent flows. If the wall heat flux in the pre-CHF region is uniform, the actual quality at the CHF location is given by the profile-fit method [26] using equilibrium qualities at the bubble detachment point and the CHF location. Once the actual quality is determined, the liquid enthalpy at the CHF location is obtained as follows:

$$h_{Lc} = [h_b - h_g x_g] / (1 - x_g) \ , \tag{38}$$

where, x_g is the local flow quality and the bulk enthalpy, h_b, is defined as

$$h_b = h_{in} + 4 L_{chf} q_{chf} / GD \ . \tag{39}$$

Here, h_{in}, L_{chf}, and D are the inlet liquid enthalpy, the heated length and diameter of flow channel. The bubble diameter at the bubble detachment point is evaluated by the modified Levy's formula of Ying and Weisman [27] and expressed by

$$D_b = \frac{0.015 \sqrt{\sigma D / \tau_w}}{\sqrt{1 + 0.1 (\rho_f - \rho_g) g D / \tau_w}} \ , \tag{40}$$

where, τ_w denotes the wall shear stress. This formula can be applicable to the system that the buoyancy effect on bubble detachment is considerable as compared with the drag force effect, such as low flow conditions.

The drag coefficient, C_D, for the vapor blanket is evaluated by the formula of Ishii and Mishima [28] for distorted bubble and expressed by

$$C_D = \tag{41}$$

$$(2/3) D_b \sqrt{(\rho_f - \rho_g) g / \sigma} \left\{ \frac{1 + 17.67 (1 - \alpha_g)^{9/7}}{18.67 (1 - \alpha_g)^{1.5}} \right\}^2$$

where, α_g is the local void fraction. The well-known void fraction and quality relationship based on the drift flux models of Chexal et al. [29] is used to find the void fraction (or quality) when the quality (or void fraction) is given. In addition to this relationship, the flow regime map is used to identify the CHF mechanism and to validate our physical model. The flow regime map is based on Mishima and Ishii's flow transition criteria [30].

3. Results and Discussion

To investigate the prediction capability of the present model and to study the parametric effect of pressure, mass flux, and inlet subcooling on the transition boiling heat flux, the comparison of the model prediction with the available experimental data of forced

convective transition boiling is performed. The experimental data of Huang et al. [31] and Weber and Johannsen [32] are selected as the representative transition boiling data.

For simulation of experimental conditions, several assumptions are needed to fit the model to the experimental procedures and conditions. Since any information for the CHF condition and the post-CHF flow regime is unavailable in the experimental sources [31, 32], it is assumed that transition boiling is prevailing in the overall heated length, and an elongated vapor blanket exists at the CHF condition whenever the inlet water flow is subcooled. The boiling curve at the mid-plane is selected as the representative boiling curve in the test section. The axial conduction due to axial temperature difference or heat flux difference is neglected in this model. The parameter ranges of the selected experimental data are listed in Table 1.

Figure 3 shows the relative contributions of macrolayer evaporation (ME) and unstable film boiling (UFB) stages to the boiling curve. In this figure, two symbolized curves designate steady-state and transient data of Huang et al. (Case A). The solid, dotted and dashed lines denote the total heat flux (given by Eq. 35) and the contributions of ME (given by Eq. 23) and UFB (given by Eq. 33), respectively. The predicted boiling curve is well matched with the steady-state data but overestimated for the transient data whose inlet flow condition is identical with the steady-state case. From this figure, it can be seen that the macrolayer evaporation dominates before the DNB temperature but rapidly decreases after the DNB temperature, while the unstable film boiling is negligible before the DNB temperature but rapidly increases with the wall superheat after the DNB temperature. Figure 4 shows the wetted area fraction predicted by this model for the above case. The wetted area fraction decreases rapidly from unity after the DNB temperature and approaches to zero near the DFB tem-

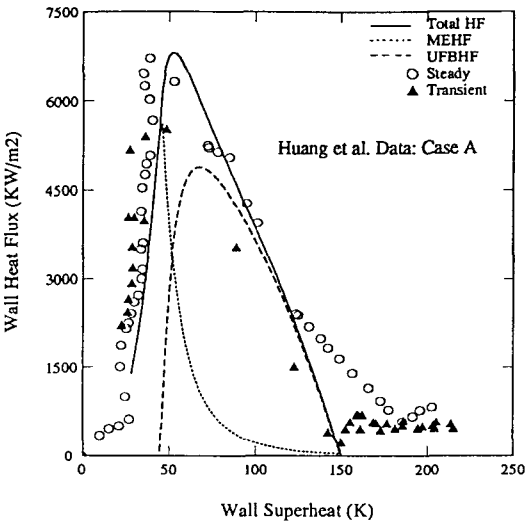

Fig. 3. Relative Contributions to Transition Boiling Heat Flux

Table 1. Parameter Range of Selected Experimental Data

Source	Huang et al. [31]			Weber & Johannsen [32]	
Range	Case A	Case B	Case C	Case D	Case E
Experiment Type	Steady-state & Transient			Steady-state	
Pressure(MPa)	0.7	1.0	1.0	0.11 – 1.0	0.7
Mass Flux (Kg/m^{2}s)	500	200	200	100	200 – 500
Inlet Subcooling (K)	5	5	15	15	5
Diameter (m)	0.01			0.01	
Length (m)	0.05			0.05	
Mid-plane	2.46 D			2.46 D	
Tube Material	Copper (heater) Monel (flow tube)			same	

perature. At the MHF point, the wetted area fraction is not about 1.0 but 0.6. This result is consistent with the experimental evidence described in the section of introduction.

Figures 5 (Case B) and 6 (Case C) show the parametric effects of inlet subcooling on the transition boiling in Huang et al. data. From this comparison, it can be seen that the inlet subcooling effect is not remarkable. In these figures, the steady-state and transient data of Huang et al. are expressed by two symbols and the prediction is depicted by the solid line. The experimental data are well predicted for the steady-state data rather than for the transient data.

Figure 7 (Case D) shows the prediction trend for

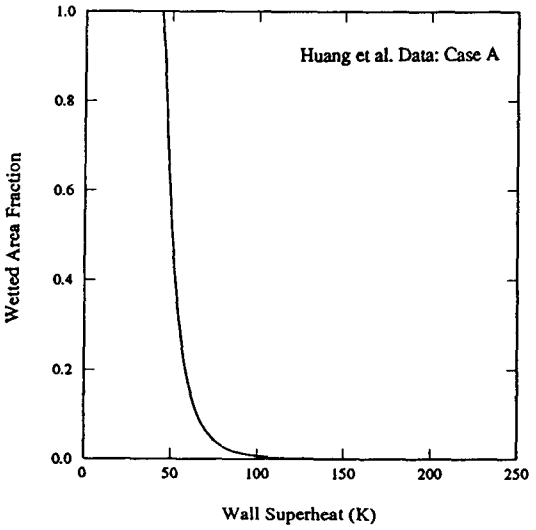

Fig. 4. Predicted Wetted Area Fraction in Transition Boiling

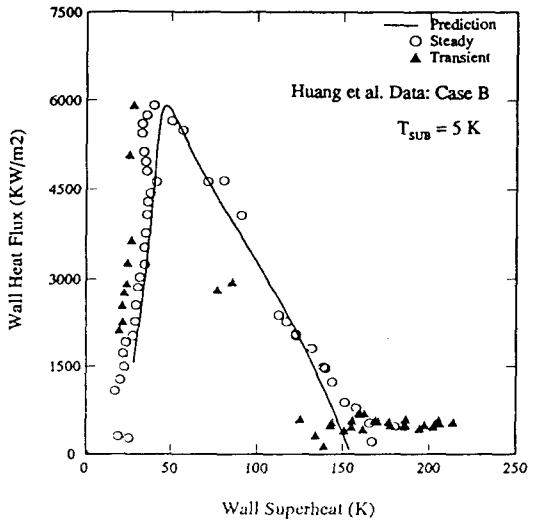

Fig. 5. Comparison of Predicted Boiling Curve with Experimental Data(Case B)

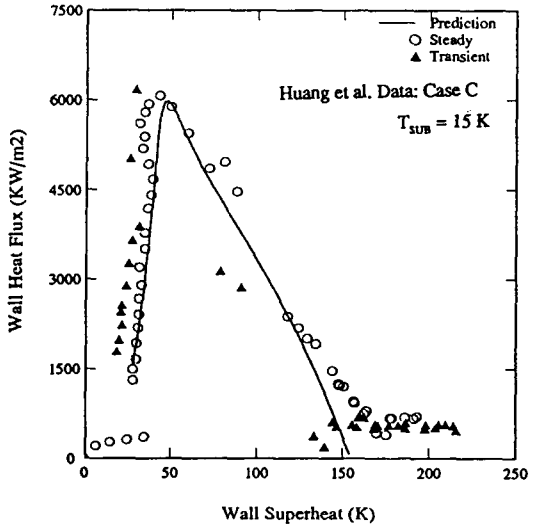

Fig. 6. Comparison of Predicted Boiling Curve with Experimental Data(Case C)

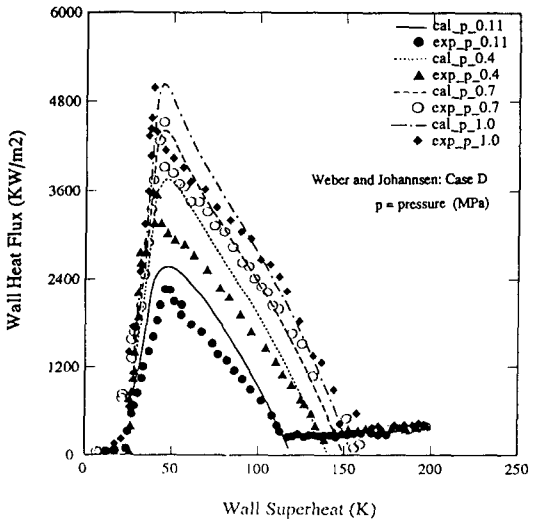

Fig. 7. Comparison of Predicted Boiling Curve with Exp. Data(Case D)

the pressure variation in Weber and Johannsen's steady-state data. The prediction is well matched with the experimental trend. However, the predictions at the low pressure cases are overestimated. This discrepancy seems to be caused by the mismatch between the physical model and the real situation. For the low pressure case, the estimated diameter and length of the vapor blanket are too large to satisfy the assumed ergodicity of the controlled phenomena. Especially, the vapor blanket length predicted by the Helmholtz instability criterion is longer than the heated length of test section. For this case, a new instability criterion is needed to avoid this problem, because the Helmholtz instability criterion derived from semi-infinite horizontal flow condition is expected to be inadequate for the cases of vertical tube with low velocity and low pressure flow. Furthermore, it is supposed that the flow regime just above the DFB temperature is an inverted annular flow according to the present physical model. However, from the installed flow regime map, the flow regime at the CHF condition was estimated as an annular flow and thus the post-CHF flow regime is expected to be a dispersed droplet flow.

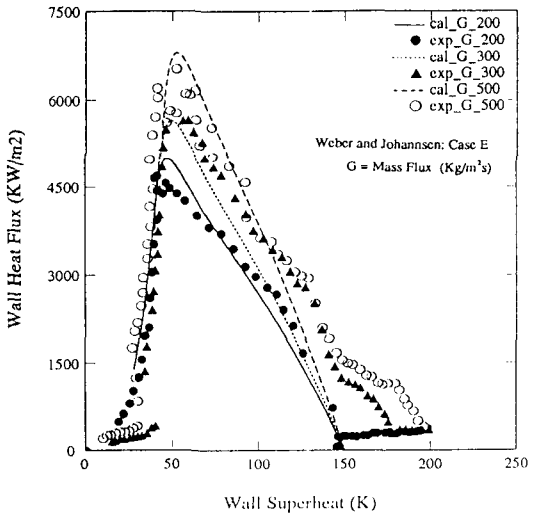

Fig. 8. Comparison of Predicted Boiling Curve with Exp. Data(Case E)

Figure 8 (Case E) shows the prediction trend for the mass flux variation in Weber and Johannsen's steady-state data. The prediction shows the same trend as the experimental data, but remarkable mismatches are observed near the DFB point. The mismatched trend near the DFB point is attributed to the weakpoint of the present unstable film boiling model, characterized by the fact that there are no par ametric factors accounting for the mass flux and inlet subcooling effects in the prediction equations for the DFB temperature and the unstable film boiling heat flux.

From the overall comparison illustrated in Figures 3 to 8, it can be concluded that the transition boiling heat fluxes including the MHF and the DFB heat flux are well predicted at low qualities/high pressures near 10 bar, while a considerable discrepancy is observed at high qualities/low pressures near the atmospheric pressure.

4. Conclusions and Recommendations

A mechanistic model for forced convective transition boiling has been developed to predict transition boiling heat flux realistically. This model is based on a postulated multi-stage boiling process occurring during the passage time of an elongated vapor blanket.

The model predictions are compared with some available experimental transition boiling data given as the steady-state or transient boiling curves. The parametric effects of pressure, mass flux and inlet subcooling on the transition boiling heat transfer are also investigated. From these comparisons, it can be seen that the transition boiling heat fluxes including the maximum heat flux and the MFB heat flux are well predicted at low qualities/high pressures near 10 bar.

From the results of model validation, the improvement directions of the present model and further studies are recommended as follows :

(1) A new hydrodynamic instabilty criterion for the determination of the vapor blanket length at low pressure and low flow condition should be estab-

lished.

(2) A generalization of the physical model for the high quality and low pressure conditions is needed.

(3) An improved model considering the parametric effects of the mass flux and inlet subcooling on the unstable film boiling heat flux and the DFB temperature is required.

(4) A two-dimensional and transient heat conduction model is needed to simulate and to evaluate the experimental condition and its data realistically.

References

1. E.K. Kalinin, I.I. Berlin and V.V. Kostiouk, "Transition Boiling Heat Transfer," Advanced Heat Transfer, 18, pp. 241−323 (1987)
2. H. Auracher, "Transition Boiling," Proc. 9th Int. Heat Transfer Conf., 1, Jerusalem, Israel, KN-5 (1990)
3. P.J. Berenson, "Experiments on Pool-Boiling Heat Transfer," Int. J. Heat Mass Transfer, 5, pp. 985−999 (1962)
4. H.S. Ragheb and S.C. Cheng, "Prediction of Transition Boiling Heat Transfer for Subcooled Water at Low Flow and Atmospheric Pressure," Multi-Phase Flow and Heat Transfer III, Part A: Fundamentals, Elsevier Pub. Co., pp. 659−669 (1984)
5. T.A. Bjornard and P. Griffith, "PWR Blowdown Heat Transfer," Symp. on Thermal and Hydraulic Aspects of Nuclear Reactor Safety, ASME, pp. 17−41 (1977)
6. Y.K. Kao and J. Weisman, "A Moving-Front Transition Boiling Model," AIChE Journal, 31, pp. 529−540 (1985)
7. H.S. Ragheb and S.C. Cheng, "Surface Wetted Area during Transition Boiling in Forced Convective Flow," J. Heat Transfer, 101, pp. 381−383 (1979)
8. D.S. Dhuga and R.H.S. Winterton, "Measurement of Surface Contact in Transition Boiling," Int. J. Heat Mass Transfer, 28, pp. 1869−1880 (1985)
9. L.Y.W. Lee, J.C. Chen, and R.A. Nelson, " Liquid-Solid Contact Measurements using a Surface Thermocouple Temperature Probe in Atmospheric Pool Boiling Water," Int. J. Heat Mass Transfer, 28, pp. 1415−1423 (1985)
10. C. Pan, J.Y. Hwang and T.L. Lin, "The Mechanism of Heat Transfer in Transition Boiling," Int. J. Heat Mass Transfer, 32, pp. 1337−1349 (1989)
11. M.T. Farmer, G.B. Jones and B.W. Spencer, "Analysis of Transient Contacting in the Low Temperature Film Boiling Regime, Part I and II," Proc., 24th Natl. Heat Transfer Conf., Pittsburgh, USA (1987)
12. Y. Katto, "A Physical Approach to Critical Heat Flux of Subcooled Flow Boiling in Round Tubes," Int. J. Heat Mass Transfer, 33, pp. 611−620 (1990)
13. C.H. Lee and I.A. Mudawwar, "A Mechanistic Critical Heat Flux Model for Subcooled Flow Boiling Based on Local Bulk Flow Conditions," Int. J. Multiphase Flow, 14, pp. 711−728 (1988)
14. I.A. Mudawwar, T.A. Incropera, and F.P. Incropera, "Boiling Heat Transfer and Critical Heat Flux in Liquid Films Falling on Vertically-mounted Heat Sources," Int. J. Heat Mass Transfer, 30, pp. 2083−2095 (1987)
15. T. Ueda and K.K. Kim, "Heat Transfer Characteristics during the Critical Heat Flux Condition in a Subcooled Flow Boiling System," Proc., 8th Int. Heat Transfer Conf., vol. 5, San Francisco, USA (1986)

16. R. Hino and T. Ueda, "Studies of Heat Transfer and Flow Characteristics in Subcooled Flow Boiling-Part I. Boiling Characteristics and Part II. Flow Characteristics, " Int. J. Multiphase Flow, 11, pp. 269−297 (1985)
17. Y. Katto, S. Yokoya, and Yasunaka, "Mechanism of Boiling Crisis and Transition Boiling in Pool Boiling," Proc. 4th Int. Heat Transfer Conf., 3, B3. 2 (1970)
18. X.C. Huang, G. Bartch, and D. Schroeder-Richter,"Quenching Experiments with a Circular Test Section of Medium Thermal Capacity under Forced Convection of Water," Int. J. Heat Mass Transfer, 37, pp. 803−818 (1994)
19. Y. Haramura and Y. Katto, "A New Hydrodynamic Model of Critical Heat Flux, Applicable Widely to Both Pool and Forced Convection Boiling on Submerged Bodies in Saturated Liquids," Int. J. Heat Mass Transfer, 26, pp. 389−399 (1983)
20. M.M Shah, "A General Correlation for Heat Transfer during Subcooled Boiling in Pipes and Annuli," ASHRAE Trans., 83, pp. 202−217 (1977)
21. B.B. Mikic and W.M. Rohsenow, "New Correlations of Pool Boiling Data Including the Effects of Heating Surface Characteristics," J. Heat Transfer, 91, pp. 245−250 (1969)
22. T. Fujita and T. Ueda, "Heat Transfer to Falling Liquid Films and Film Breakdown-II, Saturated Liquid Films with Nucleate Boiling," Int. J. Heat Mass Transfer, 21, pp. 109−118 (1978)
23. R. Mesler, "Nucleate Boiling in Thin Liquid Films," Boiling Phenomena : Physicochemical & Engineering Fundamentals and Applications, 2, Hemisphere, WA, pp. 813−819 (1979)
24. I.A. Kopchikov et al., "Liquid Boiling in a Thin Film," Int. J. Heat Mass Transfer, 12, pp. 791−796 (1969)
25. D.R.H. Beattie and K.R. Lawther, "An Examination of the Wall Temperature Drop Phenomena during Approach to Flow Boiling Crisis," Proc. 8th Int. Heat Transfer Conf., San Francisco, 4, pp. 2215−2219 (1986)
26. R.T. Lahey Jr. and F. Moody, "Two-Phase Flow (Chap. 5)," The Thermal-Hydraulics of A Boiling Water Nuclear Reactor, American Nuclear Society, pp. 173−248 (1977)
27. S.H. Ying, and J. Weisman, "Prediction of the CHF in Flow Boiling at Intermediate Qualities," Int. J. Heat Mass Transfer, 29, pp. 1639−1648 (1986)
28. M. Ishii and K. Mishima, "Two-Fluid Model and Hydrodynamic Constitutive Relations," Nucl. Engrg. Design, 82, pp. 107−126 (1984)
29. B. Chexal, et al., "A Void Fraction Correlation for Generalized Applications," Proc. 4th Int. Topical Mtg. Nuclear Reactor Thermalhydraulics (NURETH), Karlsruhe, pp. 996−1002 (1989)
30. K. Mishima and M. Ishii, "Flow Regime Transition Criteria for Upward Two-Phase Flow in Vertical Tubes," Int. J. Heat Mass Transfer, 27, pp. 723−737 (1984)
31. X.C. Huang, P. Weber, and G. Bartsch, "Comparison of Transient and Steady-State Boiling Curves for Forced Upflow of Water in a Circular Tube at Medium Pressure," Int. Comm. Heat Mass Transfer, 20, pp. 383−392 (1993)
32. P. Weber and K. Johannsen, "Convective Transition Boiling of Water at Medium Pressure," Proc. 9th Int. Heat Transfer Conf., 6, Jerusalem, Israel, pp. 35−40 (1990)